



Molten Salt Synthesis of Photocatalyst Material SrBi₄Ti₄O₁₅ for Methylene Blue Degradation

Muhammad Lathif al-Abror¹, Erna Hastuti², Anton Prasetyo^{1,*}

¹Department of Chemistry, Faculty of Science and Technology, Universitas Islam Negeri Maulana Malik Ibrahim Malang, Malang 65144, Indonesia

²Department of Physics, Faculty of Science and Technology, Universitas Islam Negeri Maulana Malik Ibrahim Malang, Malang 65144, Indonesia

*E-mail: anton@kim.uin-malang.ac.id

Article History

Received: 17 March 2022; Received in Revision: 14 December 2022; Accepted: 20 December 2022

Abstract

The four-layered Aurivillius SrBi₄Ti₄O₁₅ compound has been reported to be potentially used as a photocatalyst material. In this research, SrBi₄Ti₄O₁₅ was prepared by the molten salt method using NaCl/KCl and then used to degrade methylene blue. The analysis of sample diffractogram indicated that the SrBi₄Ti₄O₁₅ was obtained but there was still the impurities of Bi₄Ti₃O₁₂. A micrograph showed that particle shape of SrBi₄Ti₄O₁₅ is plate-like (sheets) with a lot of agglomeration. The band gap energy of SrBi₄Ti₄O₁₅ is 3.14 eV (394.85 nm), according to the Kubelka-Munk calculation from the spectrum of reflectance. The photocatalytic test results showed that SrBi₄Ti₄O₁₅ degraded methylene blue to 47.8% in 120 minutes.

Keywords: Aurivillius, degradation, methylene blue, photocatalyst material, SrBi₄Ti₄O₁₅

1. Introduction

Dye pollutants caused by industrial activities have become a global concern because of their serious environmental impact, such as carcinogenicity and inability to be decomposed by biological processes (Schwarzenbach et al., 2006; Cripps et al., 1990). Various methods have been developed to address this issue, and one of the potential methods is photocatalyst because of its low cost, chemical stability, low toxicity, and no waste generated (Fujishima et al., 2000). Methylene blue is a dye commonly used in the textile industry. Because of its complex aromatic structure, methylene blue is chemically stable and difficult to degrade via biological processes (Fadillah et al., 2018). In addition, methylene blue is toxic to humans and capable of harming aquatic ecosystems by inhibiting biota growth and chelating metal ions, making them toxic to aquatic organisms (Sheng et al., 2009). Therefore, special handling methods are required, such as the use of semiconductor photocatalysts.

One of crystal structure compound reported to be potentially used in photocatalyst technology is the Aurivillius structure family (Wang et al., 2010; Lu et al., 2015). Aurivillius compound family is a metal oxide compound consisting of a pseudo-perovskite layer (A_{n-1}B_nO_{3n+1})²⁻ and a bismuth (Bi₂O₂)²⁺ layer alternately arranged along the c axis with A is the larger cation (1.34-1.61 Å) with

dodecahedral coordination, such as Na⁺, K⁺, Ba²⁺, Pb²⁺, Bi³⁺, Sr²⁺, rare earth metals, or their mixtures, and B is a smaller cation (0.59-0.65 Å) with octahedral coordination, such as Mo⁶⁺, Ti⁴⁺, Ta⁵⁺, Nb⁵⁺, W⁶⁺, and n represent the number of pseudo perovskite layers (Borg et al., 2002). Many Aurivillius compounds can be applied as photocatalyst material, such as Bi₄Ti₃O₁₂, CaBi₂Ta₂O₉, SrBi₂Ta₂O₉, BaBi₂Ta₂O₉, and SrBi₄Ti₄O₁₅ (Li et al., 2018; Li et al., 2008; Tu et al., 2019). The photocatalytic properties of Aurivillius compounds are related to electrons in the Bi 6s and O 2p orbitals (valence band) (Wang et al., 2020). SrBi₄Ti₄O₁₅ is a four-layer Aurivillius compound with a band gap energy of 3.0 eV that has better photocatalytic activity in reducing CO₂ gas than Bi₄Ti₃O₁₂, TiO₂, and BiOBr (Tu et al., 2019). In addition, Haikal and Prasetyo (2021) also reported that SrBi₄Ti₄O₁₅ can degrade rhodamine B by 41.10% in 120 minutes. However, the photocatalyst properties of four-layer Aurivillius compound report is still limited. In addition, the activity photocatalyst of SrBi₄Ti₄O₁₅ on dye compounds degradation, such as methylene blue is still not widely reported.

One of the factors that affected the Aurivillius compound's photocatalytic activity is its particle morphology (Cheng et al., 2021). Previous studies have discovered that plate-like Aurivillius compounds are an effective photocatalysts (Liu et al., 2019; Zhao et al.,

2018). Chen et al., (2016) suggested that $\text{Bi}_4\text{Ti}_3\text{O}_{12}$ nanosheet has a good ability to degrade rhodamine B because of the high number of active sites on its surface particle, and can inhibit the rate of recombinant electrons (e^-)-hole (h^+) (Chen et al., 2016).

Many researchers have synthesized the four-layer Aurivillius compound family using various methods, such as (a) solid state reaction (Ding et al 2020) (b) molten salt synthesis (Zhao et al., 2014) (c) hydrothermal (Sardar, 2012), and sol-gel (Mamidi et al, 2018). The molten salt method has been used by many researchers to synthesize the compound $\text{SrBi}_4\text{Ti}_4\text{O}_{15}$, and to deliver typical particle morphology (Garcia-Guederrama et al., 2005; Zulhadjri et al., 2011; Kimura, 2011). In addition, the molten salt method has several advantages, such as (a) a low reaction temperature, (b) control over particle size and shape, (c) increased homogeneity, and (d) green synthesis (Kimura, 2011; Rahman, 2003).

The crystal growth process in the molten salt method is divided into two stages: (a) nucleation and (b) crystal growth. During the nucleation step, a crystal nucleus is formed and expanded through the crystal growth process (Kimura, 2011; Marela et al., 2021). In addition, the morphology of the particles obtained by the molten salt method was influenced by several factors, including the time and temperature of synthesis, the salt/product ratio, and the type of salt flux. Controlling these parameters would result in particles with distinct morphology (Akdogan et al., 2006).

Mixed salts (such as NaCl/KCl , and $\text{Na}_2\text{SO}_4/\text{K}_2\text{SO}_4$) are often used in the molten salt synthesis which aims to get lower the melting point temperature. Zhao et al (2014) synthesized plate-like $\text{Bi}_4\text{Ti}_3\text{O}_{12}$ using mixed $\text{Na}_2\text{SO}_4/\text{K}_2\text{SO}_4$ salt at temperature range 850-950 °C. It indicates that mixed salt can be used in molten salt synthesis of Aurivillius compound to produce the plate-like (sheet) particle. Chang et al. (2014) reported that they successfully synthesized $\text{SrBi}_4\text{Ti}_4\text{O}_{15}$ compound using the molten salt method, and obtained particles in the form of microplatelets (microsheets). However, studies on the use of the plate-like $\text{SrBi}_4\text{Ti}_4\text{O}_{15}$ obtained a molten salt method to degrade dye compound is still limited thus further studies are needed to reveal its photocatalyst properties. Therefore, in this research, we synthesized plate-like $\text{SrBi}_4\text{Ti}_4\text{O}_{15}$ via the molten salt method using mixed salt NaCl/KCl and investigated its

photocatalytic activity in degrading methylene blue.

2. Methodology

2.1. Materials

The chemicals used in this research were Bi_2O_3 (Himedia, 99% powder), TiO_2 (Sigma-Aldrich, 99% powder), SrCO_3 (Sigma-Aldrich, 99.9% powder), NaCl (Merck, 99%), KCl (Merck, 99%), AgNO_3 (Merck, 99%), and acetone (Merck).

2.2. Synthesis of $\text{SrBi}_4\text{Ti}_4\text{O}_{15}$

The molten salt method was used to synthesize the Aurivillius $\text{SrBi}_4\text{Ti}_4\text{O}_{15}$ compound target, with a salt mixture of NaCl/KCl (1:1) and a mole ratio of the target compound and salt of 1:7. The precursors Bi_2O_3 , TiO_2 , and SrCO_3 were mixed as the first step in the synthesis. Stoichiometrically, the precursor mass requirement was calculated with a target mass of three grams. The mixture was then ground until homogeneous with an agate mortar for one hour, with acetone added during the grinding process. The mixture was calcined for eight hours at 700°C. The mixture was then homogenized for one hour with an agate mortar using NaCl/KCl salt (salt requirement is based on stoichiometric calculations). The mixture was then re-calcined in a furnace for eight hours at 750 and 800°C. The product samples were washed with hot distilled water to remove the NaCl and KCl salts. The AgNO_3 test was used to determine the salt content of NaCl/KCl . Finally, the product was dried for three hours in a 110°C oven.

2.3. Sample Characterization

Characterization techniques used in this study included X-ray diffraction (XRD), scanning electron microscopy-energy dispersive X-ray spectroscopy (SEM-EDS) and ultraviolet-visible diffuse reflectance spectroscopy (UV-Vis DRS). The XRD instrument was used to determine the type of compound in a sample. The measurements were taken at $2\theta = 3-90^\circ$ using a Rigaku Miniflex diffractometer with a Cu K radiation source ($\lambda = 1.540593$). SEM-EDS characterization was used to analyze particle morphology, and to determine the constituent elements of a compound. This measurement was taken with a JEOL JSM-6360LA and a magnification of 15.000x. The UV-Vis DRS instrument was used to study the reflectance pattern of light, and the band gap energy would be calculated using the Kubelka-Munk equation. A Thermo Scientific Evolution

220 spectrometer with a wavelength range of 200–800 nm was used for the measurements.

2.4. Methylene Blue Degradation (Photocatalytic Activity Test)

At a concentration of 4 ppm methylene blue, 0.1 gram of $\text{SrBi}_4\text{Ti}_4\text{O}_{15}$ was added to 100 mL of methylene blue. The mixture was then stirred in the dark for 30 minutes with a magnetic stirrer to achieve adsorption-desorption equilibrium. Then, it was exposed to 8 Gaxindo T5 N093 8 Watt ultraviolet lamps in a photoreactor for 30, 60, 90, and 120 minutes. UV-Vis spectroscopy (Thermo Scientific Evolution 220 spectrometer) with a maximum wavelength of 664 nm was used to measure the concentration of methylene blue as a result of the degradation process.

3. Results and Discussion

3.1. Characterization Sample Product

Figure 1 shows the sample diffractogram, and a $\text{SrBi}_4\text{Ti}_4\text{O}_{15}$ compound was obtained based on the conformity of the peaks with the Joint Committee on Powder Diffraction Standard (JCPDS) data No.43-0973, with typical peaks at position $2\theta = 21.76, 23.1, 30.3, 32.9, 37.2, 38.7, 39.7, 47.2, 52.5, 57.2, 64.57,$ and 69.2° . Figure 1 also shows the peak diffraction shape is sharp that indicates the crystallinity of the sample is good. However, the diffractogram shows additional peaks indicating the presence of $\text{Bi}_4\text{Ti}_3\text{O}_{12}$ impurities at $2\theta = 16.3, 26.93, 48.09, 51.39,$ and 62.52° . This impurity phase is the result of a reaction between Bi_2O_3 and TiO_2 precursors that does not react with SrCO_3 .

One of the stages in the molten salt synthesis method is the rearrangement and diffusion of precursor species in the molten salt. At this stage, the reaction between the precursors has occurred in the flux salt media at above melting point of NaCl/KCl salt. As know well that the salt type influenced to the synthesis mechanism in molten salt synthesis. The presence of impurities (SrCO_3) indicates that the flux of NaCl/KCl salt (1:1) is still not suitable for making a reaction. Therefore it may SrCO_3 precursor does not diffuse well in the NaCl/KCl flux (Qiu et al., 2017).

Furthermore, the average crystallite size was determined using the Debye-Scherrer equation ($D = \frac{K\lambda}{\beta \cos \theta}$ with D is the crystallite size (nm), λ is the wavelength of X-ray source with Cu $k\text{-}\alpha$ (1.5406 nm), K is the Scherer constant (0.9), β is full width half maximum

peak (radians), and θ is diffraction angle) (Benali et al., 2020). According to the calculations, the average crystal size of the sample is ~ 80 nm.

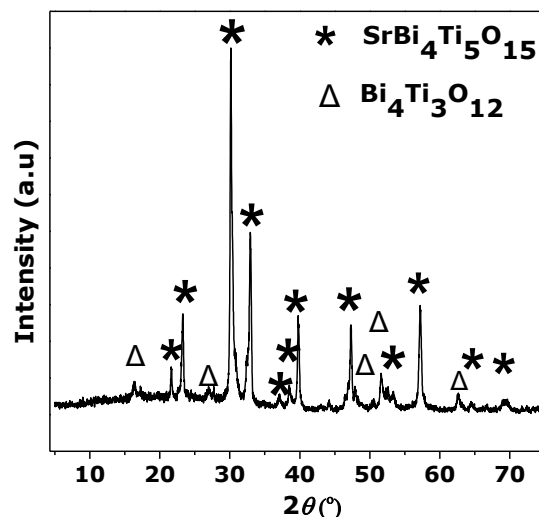


Figure 1. The diffractogram of $\text{SrBi}_4\text{Ti}_4\text{O}_{15}$.

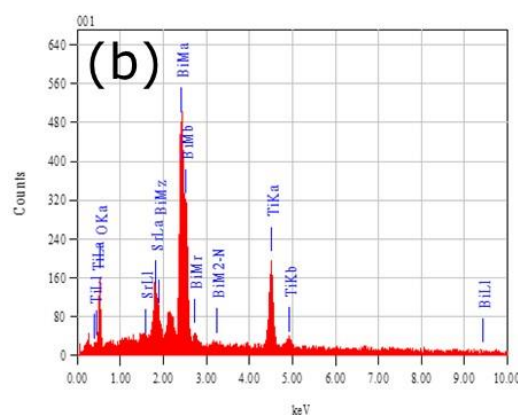
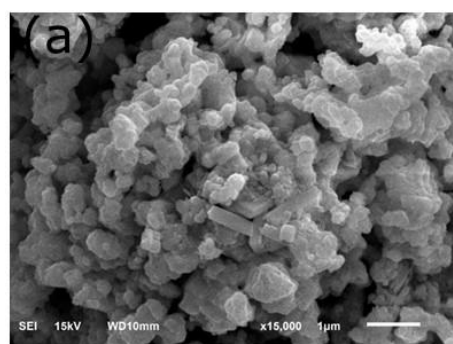


Figure 2. Micrograph and EDS spectrum of $\text{SrBi}_4\text{Ti}_4\text{O}_{15}$.

Figure 2 shows a micrograph of the $\text{SrBi}_4\text{Ti}_4\text{O}_{15}$ compound with particle size about 250-500 nm. The morphology has a plate-like shape and agglomerated particles. Figure 2 also shows that the particle size is small and

uniform relatively. It indicates that the nucleation rate is higher than the growth particle rate. The crystal seed is formed at nucleation stage therefore the higher nucleation rate produce large amounts of small-sized particles. Meanwhile the particle agglomeration due to high synthesis temperatures condition (Wang and Chen, 2012). In this research used 750 and 850 °C, meanwhile the melting point of NaCl/KCl is 657 °C. The EDS spectra (Figure (2(b)) confirms constituent elements (Sr, Bi, Ti, and O) present in the sample and there is no other element that indicates impurities. The results of percent elemental weight are summarized in Table 1.

Table 1. The EDS results.

Sample	Elemental weight (%)			
	Sr	Bi	Ti	O
SrBi ₄ Ti ₄ O ₁₅	6.75	65.62	16.49	11.14

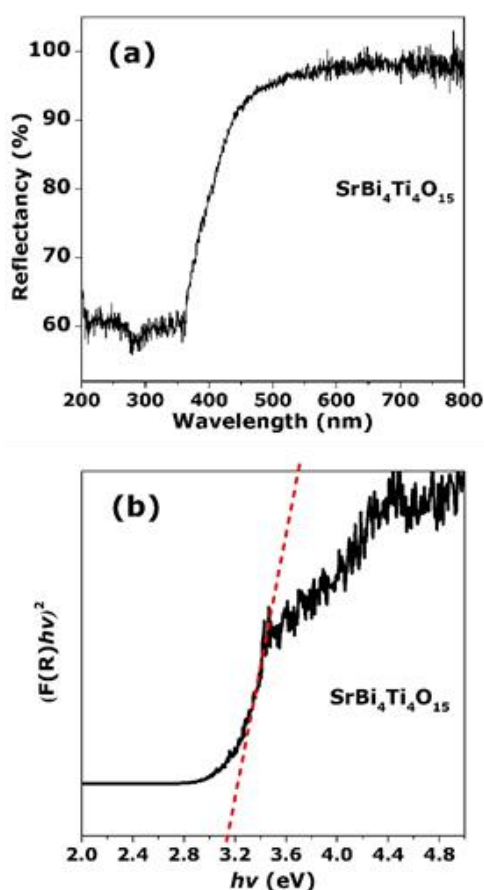


Figure 3. (a) The UV-Vis DRS spectrum, and (b) Tauc plot of SrBi₄Ti₄O₁₅.

Figure 3 shows the Kubelka-Munk equation's UV-Vis DRS spectrum and Tauc plot. According to the Kubelka-Munk calculation, the band gap energy of SrBi₄Ti₄O₁₅ is 3.14 eV, which corresponds to a wavelength of 394.85 nm. It relates to the amount of energy

required to excite electrons from the valence band (VB) in the O 2p and Bi 6s orbitals to the conduction band (CB) in the Ti 3d orbitals (Naresh and Mandal, 2014). The sample's band gap energy is higher than that reported previously by Tu et al., (2019). Impurities in the sample may influence the bandgap energy. The band gap energy obtained also shows that the SrBi₄Ti₄O₁₅ sample still works in the UV light region, and it gives a disadvantage for utilization as photocatalyst material.

3.2. Activity Photocatalyst Test

3.2.1. Adsorption-desorption test

Methylene blue degradation occurs on the surface of materials, so dye adsorption by SrBi₄Ti₄O₁₅ is a possibility. Figure 4 depicts the UV-Vis spectrum of the adsorption-desorption test, demonstrating that absorbance slightly decreases as methylene blue concentration decreases. It correlates to interaction between SrBi₄Ti₄O₁₅ surface and methylene blue. It proves that the SrBi₄Ti₄O₁₅ compound is capable of adsorbing methylene blue. SrBi₄Ti₄O₁₅ adsorption properties are comparable to those reported by Ziyaadini and Ghashang (2021), who reported the ability of Co doped SrBi₄Ti₄O₁₅ compounds to absorb Rhodamine B. They also reported that the adsorption mechanism between Rhodamine B and Co-doped SrBi₄Ti₄O₁₅ is chemical adsorption (Ziyaadini and Ghashang, 2021).

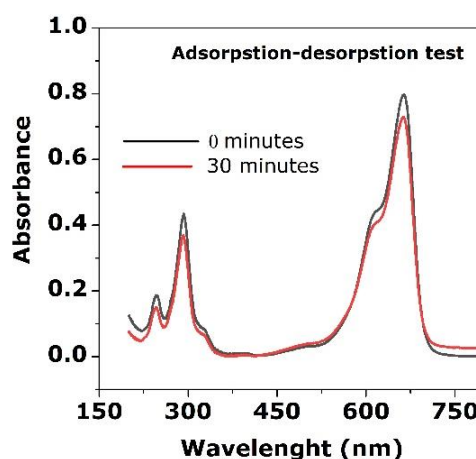


Figure 4. The spectra of adsorption-desorption test.

3.2.2 Methylene blue degradation test

The absorption spectra of methylene blue degradation by SrBi₄Ti₄O₁₅ are shown in Figure 5, and it can be seen that the absorption intensity decreases as a function of time. It indicates that methylene blue concentration decrease as a result degradation process by

$\text{SrBi}_4\text{Ti}_4\text{O}_{15}$. The calculation results of methylene blue concentration after degradation process were presented in Figure 6. According to this result, increasing the photocatalytic process time can enhance the percentage of degradation, with methylene blue being reduced up to 47.8% in 120 minutes. These results imply that the $\text{SrBi}_4\text{Ti}_4\text{O}_{15}$ photocatalyst exhibits good photocatalytic activity.

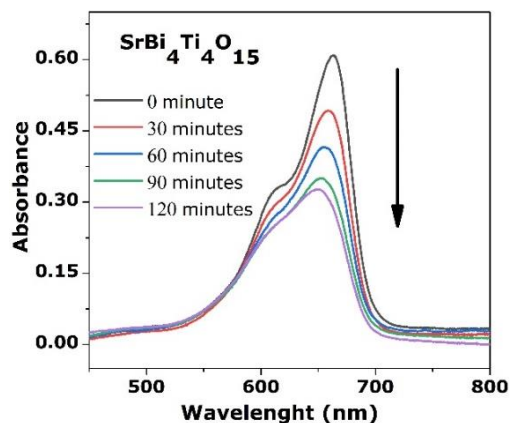


Figure 5. The absorption spectra of methylene blue degradation by $\text{SrBi}_4\text{Ti}_4\text{O}_{15}$.

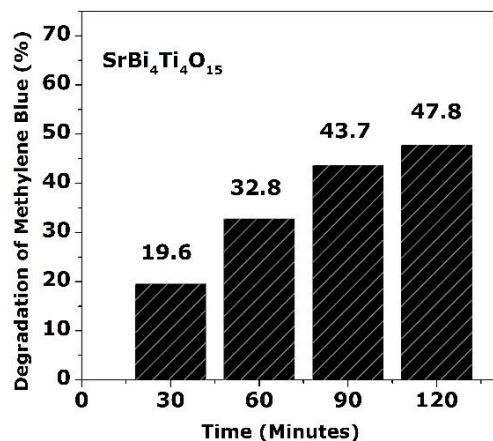


Figure 6. Percentage degradation of methylene blue by $\text{SrBi}_4\text{Ti}_4\text{O}_{15}$.

Figures 4 and 5 also suggest that the photocatalyst process plays a significant role in reducing the concentration of methylene blue because the contribution of the adsorption process to reducing the concentration of methylene blue is small. Using the dye degradation mechanism by another photocatalyst semiconductor compounds thus the degradation mechanism of methylene blue by $\text{SrBi}_4\text{Ti}_4\text{O}_{15}$ can be describe as follows: the light hit the surface of $\text{SrBi}_4\text{Ti}_4\text{O}_{15}$ as a result the electrons (e^-) move from valence band (VB) to the conduction band (CB) and cause holes (h^+) formation in the VB. Furthermore, e^- (VB) react with O_2 species to form O_2^- superoxide anion ($\text{O}_2^{\cdot-}$),

while h^+ (CB) react with $\text{OH}/\text{H}_2\text{O}$ to form OH radical (OH^\cdot). Then, the existence of radicals reacts with dyes compound and produced new smaller molecule (methylene blue degradation) (Cheng et al., 2021 and Mamidi et al., 2019)

When compared to $\text{Bi}_4\text{V}_2\text{O}_{11}$ (some other Aurivillius compound), the degradation ability of $\text{SrBi}_4\text{Ti}_4\text{O}_{15}$ compounds is lower, which is possible because of (a) the lower bandgap energy of $\text{Bi}_4\text{V}_2\text{O}_{11}$ (2.08 eV), (b) the smaller particle size of $\text{Bi}_4\text{V}_2\text{O}_{11}$, it can be explained because the dye degradation process occurs on the surface of photocatalyst compound thus the larger of surface area give the higher degradation ability. (Lu et al., 2015), and (c) the $\text{SrBi}_4\text{Ti}_4\text{O}_{15}$ particle in agglomerated form. Meanwhile, Pellegrino et al., (2017) suggested that the agglomeration particles can interfere with the absorption process of photon radiation, then causing the photocatalytic activity to decrease (Pellegrino et al., 2017). The another factor affected to photocatalysts activity is e^-h^+ recombination rate that correlates the life time of e^-h^+ (Chen et al., 2016). Meanwhile the existence of e^-h^+ is very important factor in dyes compound degradation, but in this research did not conduct the photoluminescence (PL) spectroscopy measurement. Thus there is no information about the influence of e^-h^+ recombination rate to methylene blue degradation result.

4. Conclusion

The compound $\text{SrBi}_4\text{Ti}_4\text{O}_{15}$ was successfully synthesized, but an impurity phase of $\text{Bi}_4\text{Ti}_3\text{O}_{12}$ was discovered that indicates the synthesis condition did not enough to reaction accomplish. The morphology of the $\text{SrBi}_4\text{Ti}_4\text{O}_{15}$ compound that was synthesized was plate-like with many agglomerations. The higher synthesis temperature may induce the agglomeration formed. The $\text{SrBi}_4\text{Ti}_4\text{O}_{15}$ compound has a bandgap energy of 3.14 eV (394.85 nm). The difference band gap energy obtained sample with previous report band gap energy of $\text{SrBi}_4\text{Ti}_4\text{O}_{15}$ due to the existence of impurities phase in the sample. The photocatalytic activity test in degrading methylene blue up to 47.8 % in 120 minutes. Despite the $\text{SrBi}_4\text{Ti}_4\text{O}_{15}$ compound can act as an adsorbent but the role of the photocatalyst mechanism is more powerful.

Acknowledgement

The authors are grateful to Isnaeni Hartiningsih, S.Si for the assistance on photocatalytic activity test.

References

- Akdogan, E.K., Brennad, R.E., Allahverdi, M., Safari, A., 2006. Effects of molten salt synthesis (MSS) parameters on the morphology of $\text{Sr}_3\text{Ti}_2\text{O}_7$ and SrTiO_3 seed crystals. *J. Electroceram.* 16, 159-165. <https://doi.org/10.1007/s10832-006-6243-2>
- Benali, E.M., Benali, A., Bejar, M., Dhahri, E., Graca, M.P.F., Valente, M.A., Costa, B.F.O., 2020. Effect of synthesis route on structural, morphological, Raman, dielectric, and electric properties of $\text{La}_{0.8}\text{Ba}_{0.1}\text{Bi}_{0.1}\text{FeO}_3$. *J. Mater. Sci: Mater Electron.* 31, 3197-3214. <https://doi.org/10.1007/s10854-020-02867-0>
- Borg, S., Svensson, G., Bovin, J.O., 2002. Structure study of $\text{Bi}_{2.5}\text{Na}_{0.5}\text{Ta}_2\text{O}_9$ and $\text{Bi}_{2.5}\text{Na}_{m-1.5}\text{Nb}_m\text{O}_{3m+3}$ by neutron powder diffraction and electron microscopy. *J. Solid State Chem.* 167, 86-96. <https://doi.org/10.1006/jssc.2002.9623>
- Chang, Y., Wu, J., Yang, B., Zhang, S., Lv, T., Cao, W., 2014. Synthesis, and properties of high aspect ratio $\text{SrBi}_4\text{Ti}_4\text{O}_{15}$ microplatelets. *Mater. Lett.* 129, 126-129. <https://doi.org/10.1016/j.matlet.2014.05.014>
- Chen, Z., Jiang, H., Jin, W., Shi, C., 2016. Enhanced photocatalytic performance over $\text{Bi}_4\text{Ti}_3\text{O}_{12}$ nanosheets with controllable size and exposed {0 0 1} facets for rhodamine B degradation. *Appl. Catal.* 180, 698-706. <https://doi.org/10.1016/j.apcatb.2015.07.022>
- Cheng, T., Sun, X., Xian, T., Yi, Z., Li, R., Wang, X., Yang, H., 2021. Tert-butylamine/oleic Acid-assisted morphology tailoring of hierarchical $\text{Bi}_4\text{Ti}_3\text{O}_{12}$ architectures and their application for photodegradation of simulated dye wastewater. *Opt.* 11, 1-11. <https://doi.org/10.1016/j.optmat.2020.10781>
- Cripps, C., Bumpus, J.A., S. Aust, S.D., 1990. Biodegradation of azo and heterocyclic dyes by phanerochaete chrysosporium. *Appl. Environ. Microbiol.* 56, 1114-1118. <https://doi.org/10.1128/aem.56.4.1114-1118.1990>
- Ding, Z.Z., Tang, X.Q., Ren, J.C., Liu, X.Z., Chen, Y.K., Xia, Z.Y., Cao, L., Chen, X.Q., 2020. Tuning the band gaps of ferroelectric Aurivillius compounds by transition metal substitution. *Ceram. Int.* 46, 8314-8319. <https://doi.org/10.1016/j.ceramint.2019.12.062>
- Fadillah, G., Putri, E.N.K., Febrianastuti, S., Munawaroh, H., Purnawan, C., Wahyuningsih, S., 2018. α -Keratin/Alginate biosorbent for removal of methylene blue on aqueous solution in a batch system. *IOP Conf. Ser. Mater. Sci. Eng.* 333. <http://dx.doi.org/10.1088/1757-899X/333/1/012052>
- Fujishima, A., Rao, T.N., Tryk, D.A., 2000. Titanium dioxide photocatalysis. *J. Photochem. Photobiol.* 1, 1-21. [https://doi.org/10.1016/S1389-5567\(00\)00002-2](https://doi.org/10.1016/S1389-5567(00)00002-2)
- Garcia-Guaderrama, M., Fuentes, L., Montero-Cabrera, M.E., Marquec-Luzera, A., Villafuerte-Castrejon, E., 2005. Molten salt synthesis and crystal structure of $\text{Bi}_5\text{Ti}_3\text{FeO}_{15}$. *Integr. Ferroelectr.* 71, 233-239. <http://dx.doi.org/10.1080/10584580590965401>
- Haikal, F., Prasetyo, A., 2021. Uji aktivitas fotokatalis senyawa aurivillius lapis empat $\text{SrBi}_4\text{Ti}_4\text{O}_{15}$ dalam mendegradasi rhodamine-B. *Al-Kimiya: Jurnal Ilmu Kimia dan Terapan.* 8, 37-41.
- Kimura, T., 2011. Molten salt synthesis of ceramic powders advances in ceramics synthesis and characterization, Processing and Specific Applications. In Tech, Rijeka. <http://dx.doi.org/10.5772/20472>
- Li, N., Wu, J., Fang, H.B., Zhang, X.H., Zheng, Y.Z., Tai, X., 2018. Au-nanorod-anchored {001} facets of $\text{Bi}_4\text{Ti}_3\text{O}_{12}$ nanosheets for enhanced visible-light-driven photocatalysis. *Appl. Surf. Sci.* 448, 41-49. <https://doi.org/10.1016/j.apsusc.2018.04.066>
- Li, Y., Chen, G., Zhang, H., Li, Z., Sun, J., 2008. Electronic structure and photocatalytic properties of $\text{ABi}_2\text{Ta}_2\text{O}_9$ (A= Ca, Sr, Ba). *J. Solid State Chem.* 181, 2653-2659. <https://doi.org/10.1016/j.jssc.2008.05.020>

- Liu, X., Zhou, Z., Lu, Y., Wang, T., Huo, P., Yan, Y., 2019. Increasing visible-light absorption for photocatalysis with black 2D Bi₄Ti₃O₁₂ nanosheets. *Adv Powder Technol.* 30, 1043–1050. <https://doi.org/10.1016/j.appt.2019.02.019>
- Lu, Y., Pu, Y., Wang, J., Qin, C., Chen, C., Seo, H. J., 2015. On structure and methylene blue degradation activity of an aurivillius-type photocatalyst of Bi₄V₂O₁₁ nanoparticles. *Appl. Surf. Sci.* 347, 719–726. <https://doi.org/10.1016/j.apsusc.2015.04.164>
- Mamidi, S., Gundeboina, R., Kurra, S., Velchuri, R., Muga, V., 2018. Aurivillius family of layered perovskites, BiREWO₆ (RE = La, Pr, Gd, and Dy): synthesis, characterization, and photocatalytic studies. *C. R. Chim.* 21, 547–552. <https://doi.org/10.1016/j.crci.2018.01.011>
- Marela, S.D., Aini, N., Hardian, A., Suendo, V., Prasetyo, A., 2021. The effect of synthesis temperature on the plate-like particle of Bi₄Ti₃O₁₂ obtained by molten nacl salt method. *Int. Res. J. Pure Appl. Chem.* 10, 64–71. <http://dx.doi.org/10.21776/ub.jpacr.2021.010.01.570>
- Naresh, G., and Mandal, T. K., 2014. Excellent sun-light-driven photocatalytic activity by aurivillius layered perovskites, Bi_{5-x}La_xTi₃FeO₁₅ (x = 1, 2). *ACS Appl. Mater. Interfaces.* 6, 21000–21010. <http://dx.doi.org/10.1021/am505767c>
- Pellegrino, F., Pellutiè, L., Sordello, F., Minero, C., Ortel, E., Hodoroaba, V., Maurino, V., 2017. Influence of agglomeration and aggregation on the photocatalytic activity of TiO₂ nanoparticles. *Appl. Catal.* 216, 80–87. <https://doi.org/10.1016/j.apcatb.2017.05.046>
- Qiu, W., Liu, Y., Ye, J., Fan, H., Wang, G., 2017. Molten salt synthesis and growth mechanism of WC platelet powders. *Powder Technol.* 310, 228–233. <https://doi.org/10.1016/j.powtec.2016.12.036>
- Rahman, M.N., 2013. *Ceramic Processing and Sintering*, Marcel Dekker Inc., New York.
- Sardar, K., Walton, R.I., 2012. Hydrothermal synthesis map of bismuth titanates. *J. Solid State Chem.* 189, 32–37. <https://doi.org/10.1016/j.jssc.2012.01.017>
- Schwarzenbach, R.P., Escher, B.I., Fenner, K., Hofstetter, T.B., Johnson, C.A., Gunten, U.V., Wehrti, B., 2006. The challenge of micropollutants in aquatic systems. *Science.* 313, 1072–1077. <https://doi.org/10.1126/science.1127291>
- Sheng, J., Xie, Y., Zhou, Y., 2009. Adsorption of methylene blue from aqueous solution on pyrophyllite. *Appl. Clay Sci.* 46, 422–424. <https://doi.org/10.1016/j.clay.2009.10.006>
- Tu, S., Zhang, Y., Reshak, A.H., Auluck, S., Ye, L., Han, X., Ma, T., Huang, H., 2019. Ferroelectric polarization promoted bulk charge separation for highly efficient CO₂ photoreduction of SrBi₄Ti₄O₁₅. *Nano Energy.* 56, 840–850. <https://doi.org/10.1016/j.nanoen.2018.12.016>
- Wang, C., and Chen, S.H., 2012. Factors influencing particle agglomeration during solid-state sintering. *Acta Mechanica Sinica.* 28, 711–719. <http://dx.doi.org/10.1007/s10409-012-0029-3>
- Wang, D., Tang, K., Liang, Z., Zheng, H., 2010. Synthesis, crystal structure, and photocatalytic activity of the new three-layer Aurivillius phases, Bi₂ASrTi₂TaO₁₂ (A= Bi, La). *J. Solid State Chem.* 183, 361–366. <https://doi.org/10.1016/j.jssc.2009.11.018>
- Wang, Y., Zhang, M., Wu, J., Hu, Z., Zhang, H., Yan, H., 2020. Ferroelectric and photocatalytic properties of Aurivillius phase Ca₂Bi₄Ti₅O₁₈. *J. Am. Ceram. Soc.*, 104, 322–328. <http://dx.doi.org/10.1111/jace.17466>
- Zhao, X., Yang, H., Li, S., Cui, Z., Zhang, C., 2018. Synthesis and theoretical study of large-sized Bi₄Ti₃O₁₂ square nanosheets with high photocatalytic activity. *Mater. Res. Bull.* 107, 180–188. <https://doi.org/10.1016/j.materresbull.2018.07.018>

- Zhao, Z., Li, X., Ji, H., Deng, M., 2014. Formation Mechanism of Plate-like $\text{Bi}_4\text{Ti}_3\text{O}_{12}$ Particles in Molten Salt Fluxes, *Integr. Ferroelectr.* 154, 54–158. <http://dx.doi.org/10.1080/10584587.2014.904705>
- ZiYaadini, M., and Ghashang, M., 2021. Removal of rhodamine B from aqueous solution using $\text{SrCo}_x\text{Bi}_4\text{Ti}_{4-x}\text{O}_{15}$ aurivillius phase ceramics. *Inorg. Nano-Met. Chem.* 51, 1-10. <http://dx.doi.org/10.1080/24701556.2020.1835973>
- Zulhadjri, Prijamboedi, B., Nugroho, A.A., Mufti, N., Fajar, A., Palstra, T.T.M., Ismunandar, 2011. Aurivillius phases of $\text{PbBi}_4\text{Ti}_4\text{O}_{15}$ doped with Mn^{3+} synthesized by molten salt technique: structure, dielectric, and magnetic properties, *J. Solid State Chem.* 184, 1318–1323. <https://doi.org/10.1016/j.jssc.2011.03.044>